Smart Structures Systems, *Vol. 20, No. 6 (2017) 769-780*
DOI: https://doi.org/10.12989/sss.2017.20.6.769

Optimal sensor placement for cable force monitoring using spatial correlation analysis and bond energy algorithm

Shunlong Li[*1], Jialin Dong[2], Wei Lu[3], Hui Li[1], Wencheng Xu[4] and Yao Jin[4]

[1]Department of Bridge and Tunnel engineering, Harbin Institute of Technology, 73 Huanghe Road, Harbin 150090, China
[2]Zhejiang Scientific Research Institute of Transport, 188 Gangyang, Hangzhou 311305, China
[3]Department of Civil and Environment Engineering, Harbin Institute of Technology (Shenzhen), HIT Campus of Xili University Town, Shenzhen 518055, China
[4]CCCC Highway Consultants CO., Ltd. (HPDI), 85 Deshengmenwai Street, Beijing 100000, China

(Received April 21, 2017, Revised October 12, 2017, Accepted November 14, 2017)

Abstract. Cable force monitoring is an essential and critical part of the safety evaluation of cable-supported bridges. A reasonable cable force monitoring scheme, particularly, sensor placement related to accurate safety assessment and budget cost-saving becomes a major concern of bridge administrative authorities. This paper presents optimal sensor placement for cable force monitoring by selecting representative sensor positions, which consider the spatial correlativeness existing in the cable group. The limited sensors would be utilized for maximizing useful information from the monitored bridges. The maximum information coefficient (MIC), mutual information (MI) based kernel density estimation, as well as Pearson coefficients, were all employed to detect potential spatial correlation in the cable group. Compared with the Pearson coefficient and MIC, the mutual information is more suitable for identifying the association existing in cable group and thus, is selected to describe the spatial relevance in this study. Then, the bond energy algorithm, which collects clusters based on the relationship of surrounding elements, is used for the optimal placement of cable sensors. Several optimal placement strategies are discussed with different correlation thresholds for the cable group of Nanjing No.3 Yangtze River Bridge, verifying the effectiveness of the proposed method.

Keywords: structural health monitoring (SHM); spatial correlation; bridges; optimum design; sensor/sensor placement

1. Introduction

Cables, including stay cables and suspenders, usually serve as critical and vulnerable structural components in long span cable-supported bridges, such as a cable-stayed bridge, suspension bridge, arch bridge, etc. 48% among over 30 cable-stayed bridges built between 1970s and 1990s in the mainland of China have been reinforced, repaired, or even removed, due to cable deterioration. And the cables of over 10 cable-stayed bridges built after 1990s need to be replaced. In recent years, more than 10 catastrophic accidents were caused by the fracture of cables or suspenders. Cable force is an important parameter to assess the health status of a cable-supported bridge, providing basic evidence for condition assessments. Thus, cable force monitoring has become an indispensable part of a structural health monitoring system for cable-supported bridges.

At present, there are two practical methods for cable force monitoring in the Structural Health Monitoring (SHM) system. The first one is recording time-varying real time cable force directly by measurement devices, such as anchor load cells (Jemielniak 1999), magneto-elastic (EM) sensors (Wang *et al.* 1999), optical fibre Bragg grating (OFBG) based smart cables (Li *et al.* 2011, Li *et al.* 2009) and so on, which have been installed on cables in some newly built bridges. The other is to identify the cable frequencies using transverse acceleration. Then, obtain the cable forces, utilizing the relationship between cable frequencies and cable force. With the development of construction technology, cable-supported bridge spans are getting increasingly longer, and the number of corresponding cables has increased to over two hundred. For example, the number of cables for the Suzhou-Nantong Yangtze River Bridge (the second longest cable-stayed bridge) is up to 272. Obviously, the most accurate, but expensive, choice would be to install sensors on all cables neglecting spatial correlation and redundancy, resulting in investment waste and data analysis difficulty. Reasonably, in a practical application, cables should be chosen in a representative section for the installation of sensors, and the rules for optimal sensor placement should be clarified. Cable sensor placement is required to include all possible cable specifications to make monitoring data more representative and practical. Otherwise, the limited information would not meet the requirements of a comprehensive safety evaluation for the cables and bridge, as a whole. On the other hand, the cables, especially those in symmetrical or adjacent positions, seem to have similar cable force variations at the same time. Taking the above two aspects into consideration, it is possible to optimize the sensor layout based on a spatial correlation between the cable forces; aiming at effectively obtaining more cable

∗Corresponding author, Associate Professor
E-mail: lishunlong@hit.edu.cn

http://www.techno-press.com/journals/sss&subpage=7
ISSN: 1738-1584 (Print), 1738-1991 (Online)

tension information and evaluating the cable group health status by limited sensors.

Sensor placement optimization was firstly studied in the field of dynamic control and system identification of spacecraft (Udwadia 2010, Lim 2012), and then, applied to modal identification and damage detection in structural engineering, structural health monitoring, etc. Numerous optimal sensor placement methods were proposed based on modal testing and parameter identification in the last decades. These can be divided into the following four categories in terms of performance criteria: (1) minimum identification error based approaches, among which the effective independence (EI), developed by Kammer (1990), Yao *et al.* (1992), is widely used, tending to maximise the determinant of the Fisher information matrix (FIM); (2) energy-driven methods, including the kinetic energy method (KEM) (Li *et al.* 2007), eigenvalue vector product (EVP) (Doebling 1995) and non-optimal driving point (NODP) (Dewolf and Zhao 1999), the most famous KEM placed sensors in a position with relatively larger modal strain energy, consistent with the position reflecting larger structural response; (3) model reduction method, proposed by Guyan (1965), achieves the purpose of refining the model by retaining the main degrees of freedom and removing secondary degrees of freedom. When used in optimal point selection, the main degrees of freedom would be selected as measuring points through successive iteration; (4) modal assurance criterion (MAC), introduced by (Allemang and Brown 1982), is also one of the most important criterion in optimal sensor placement, and the mass-weighted MAC are recommended as a validation criterion (Penny *et al.* 1994). The principle to minimize the off diagonal terms of the MAC matrix (Carne and Dohrmann 1995), as well as minimize the average of the off-diagonal elements and highest value of the MAC matrix (Liu *et al.* 2008) was proposed for optimal sensor position selection. Other than the aforementioned approaches, certain other optimal methods were proposed based on spline function interpolation (Baruh and Choe 1987) and observability (Waldraff *et al.* 1998). Among these optimal sensor placement methods, the most commonly used criterion would be dynamical property based. To improve the performance of sensor placement, optimization algorithms, such as genetic algorithm (GA), (Lu *et al.* 2015, Jung *et al.* 2016), multi-objective genetic algorithm, (Nestorovic *et al.* 2015), as well as simulated annealing (SA) algorithm (Tong *et al.* 2014) are employed to determine the sensor positions. Some optimization algorithms have also been proposed to improve the traditional coding methods in sensor optimization, such as distributed monkey algorithm (DMA) (Yi *et al.* 2015), virus monkey algorithm (VMA) (Yi *et al.* 2015), the nondirective movement glowworm swarm optimization (NMGSO) algorithm (Zhou *et al.* 2015). In recent years, methods based on spare component analysis (SCA) (Yang and Nagarajaiah 2013), sparse representation (SR) and compressed sensing (CS) (Yang and Nagarajaiah 2014), complexity pursuit (CP) (Yang and Nagarajaiah 2013) has also been proposed for output-only modal identification, multiple damage identification when the limited sensors can not meet the requirement of traditional approaches. However, literatures on the use of the spatial correlation of mechanical properties for optimal cable force sensor placement are currently limited. Even the law of spatial correlation between cables could not clearly be described for lack of massive monitored cable force datasets.

In this study, the inherent spatial correlativeness between cables, summarized by long-term monitoring cable force datasets, were first, introduced, and then, reasonable cable force sensor arrangements were optimized by the bond energy algorithm. The paper is organized as follows: In section 2, different correlation analysis methods including the Pearson coefficient, maximal information coefficient (MIC) and mutual information (MI), were all employed and discussed for detecting the potential correlation between cables, selecting the most suitable indicator for spatial correlation. The bond energy algorithm, sensor classification principle, and optimal point selection are mainly introduced in section 3. Moreover, the proposed methodology with mutual information is applied to cables on the Nanjing No.3 Yangtze River Bridge, and several optimal schemes under the corresponding correlation threshold verify the effectiveness of the proposed approach. Finally, conclusions and suggestions are given in section 4.

2. Spatial correlation detection and description between cables

Nanjing No.3 Yangtze River Bridge is one of the longest cable-stayed bridges in China, comprised of two towers and four cable planes. The span of the bridge is arranged as 63 m+257 m+648 m+257 m+63 m, as shown as Fig. 1. The structural health monitoring system was established in 2006, involving several monitoring items related to bridge structural safety, such as environmental and load conditions (temperature, humidity, wind and vehicle loads), global responses (displacement, acceleration of bridge deck and tower), and local responses (strain, cable forces, support reaction). Particularly, all 168 high-strength parallel steel cables of the bridge had anchor load cells installed to monitor the real-time tension with a sampling frequency of 2 Hz. Thus, the cable force datasets, monitored for approximately 5 years, provide a solid basis for detecting the hidden spatial correlation in the cable group. 84 cables on the upriver were selected and discussed in this paper, marked as 1~84 from the side span of the north tower to the side span of south tower. The 84 investigated cable force datasets also show that more than one-third of the anchor load cells malfunctioned or were dead after 5 years of operation. As far as we know, anchor load cells replacement always leads to complicated calibration and adjustment, which consumes a large amount of money and time. Thus, vibration based cable force identification has become the most appreciated choice for administrative authority of this bridge because of the mature and reliable manufacture, and easy installation and replacement for accelerators. Then, a cost-effective cable accelerometer replacement scheme becomes a main concern of the bridge

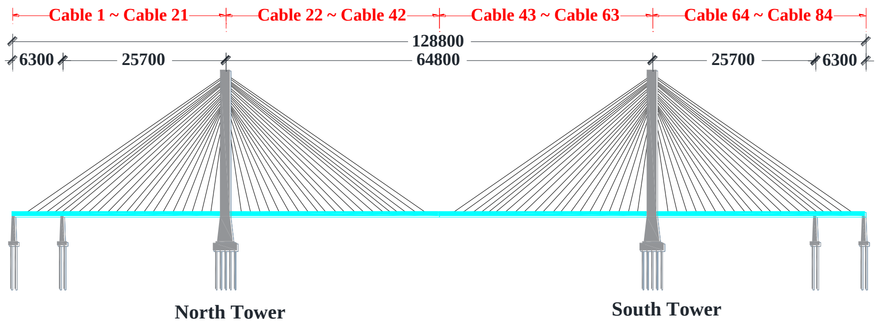

Fig. 1 General description of Nanjing No.3 Yangtze River Bridge (Unit: cm)

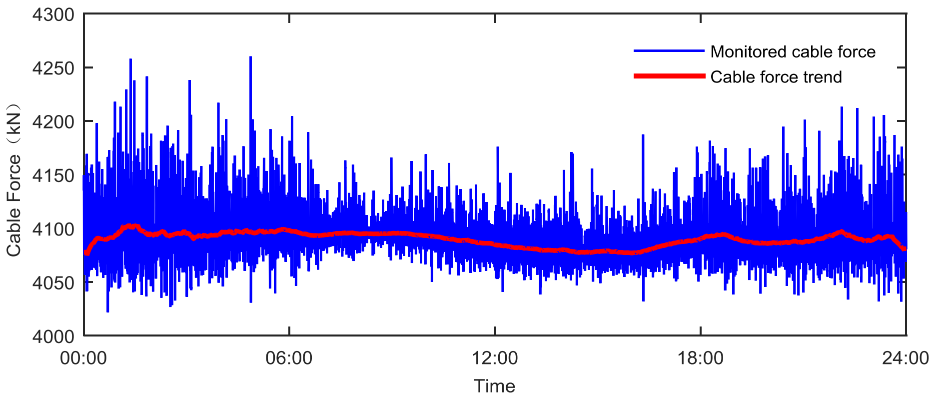

Fig. 2 Extraction of cable force trend from monitored data (00:00-24:00 June 1, 2006)

authority, especially utilizing the monitored cable force datasets and verifying the effectiveness and significance of their monitoring management and maintenance.

2.1 Pre-processing of monitored cable forces

The monitored cable force is mainly induced by three parts: dead load, environmental loads, and vehicle loads, expressed as Eq. (1).

$$T = T_i + T_e + T_v \tag{1}$$

where T, T_i, T_e, and T_v indicate the monitored cable force, dead load induced cable force, environment load induced cable force, especially temperature load induced cable force, as well as vehicle load induced cable force, respectively.

Due to the complicated random distribution of vehicles on the bridge, it is difficult to logically describe the association between the monitored cable forces directly. Therefore, cable forces caused by dead load and ambient factors, mainly by temperature load, was employed for this study as the vibration based cable force identification method could obtained similar cable force patterns.

In this study, the B-spline interpolation method (Mehrad *et al.* 2013) based on the data local feature is adopted to extract the cable force trend from monitored datasets, where the peaks after median filtering are regarded as characteristic points of B-spline interpolation. The interpolating curve was considered as the cable force trend, mainly caused by dead load and temperature load, which shows a different variation characteristic from vehicle load induced cable forces. The representative monitored cable force, as well as extracted cable force trend is shown in Fig. 2.

Considering the relative stability of data collection and transmission of the SHM system since the opening of the bridge, the 84 investigated cable forces on the upriver side from June 2006 to February 2007 were selected in this paper, and the mean value of the cable force trend at each half-hour time segment was adopted for subsequent analysis. Therefore, a dataset $\mathbf{X} = \begin{bmatrix} x_1 & x_2 & \cdots & x_{84} \end{bmatrix} \in \Re^{6120\times 84}$, with 6120 data points after removing missing data and erroneous data caused by acquisition system, was obtained, where x_i indicates the monitored ith cable force trend.

Usually, for the two arbitrary cable force trend datasets x_i and x_j at different positions, the spatial correlation degree $Corr(x_i, x_j)$ could be conducted by Pearson coefficients

$$Corr(x_i, x_j) = \frac{Cov(x_i, x_j)}{\sqrt{Var(x_i, x_j)Var(x_i, x_j)}} \tag{2}$$

where $Cov(\cdot)$ and $Var(\cdot)$ indicate the covariance and variance computation formulations.

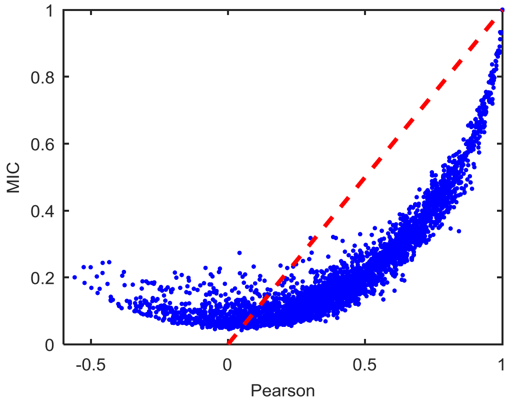

Fig. 3 Comparison between MIC and Pearson coefficients

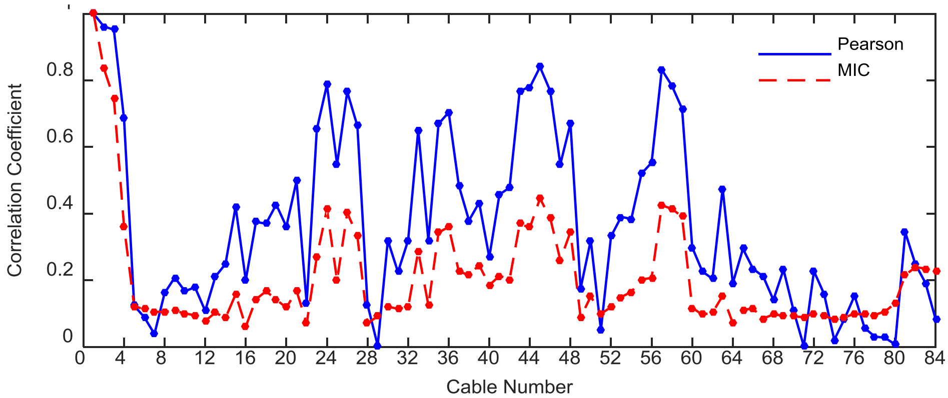

Fig. 4 Correlation coefficient of Cable 1 with other 83 cables

The complexity of the actual bridge and uncertainty of actual loading conditions lead to the fact that correlation between monitored cable forces might not be described by a simple linear relationship, $Corr(x_i, x_j)$. The MIC and MI were employed to investigate the appreciated dependence measure for monitored cable force trend datasets. The correlation value is a non-dimensional parameter ranged from -1 to 1. The absolute correlation value varies from 0 to 1, demonstrating that the dependence between two parameters varies from weakest to closest.

2.2 Spatial correlation analysis using MIC

The MIC introduction by Reshef *et al.* in 2011 (Reshef, *et al*. 2011), as a measure of dependency between variables, can describe a wide range of association, both functional and non-functional, and is called “A correlation for 21st century” (Speed 2011). For a set of ordered pairs D, an x-by-y grid G is produced by parting the x-values of D into x bins and y- values into y bins (possible with empty bins). D_G denotes the probability distribution induced by grid G, where the probability refers to the proportion to the number of data points falling into each box. $I(\cdot)$ denotes the mutual information for every grid and $I^*(D,x,y)=\max_G I(D|_G)$ represents the maximal value for each pair integer (x, y) in a x-by-y grid. MIC is defined as

$$MIC(D)=\max_{xy<B(n)}\frac{I^*(D,x,y)}{\log_2 \min\{x,y\}} \tag{3}$$

where threshold B is a function of sample size and is recommended as $B=n^{0.6}$.

For the 84 investigated cables, the MIC and Pearson correlation matrix can be calculated and illustrated as $\mathbf{M}=\left[MIC_{ij}\right]_{84\times84}$ and $\mathbf{R}=\left[Corr_{ij}\right]_{84\times84}$. The scatter plot of two correlation matrices is shown in Fig. 3, where the red line indicates that the MIC equals the Pearson coefficient. It can be seen from Fig. 3 that most MIC with the default threshold setting $B=n^{0.6}$ were below the red line, indicating that most MIC were smaller than the Pearson coefficients for investigated cable forces. Moreover, the MIC shows no significant advantage over Pearson coefficients in detecting deep nonlinear correlation with default settings.

Take Cable 1 for further investigation. The comparison of two coefficients, calculated by Cable 1 with the other 83 cables, is shown in Fig. 4. The Pearson coefficients and MIC had basically the same variation trend and most Pearson coefficients were greater than MIC. This further demonstrates that MIC does not reflect superiority in describing the relationship between monitored cable force trends with the default setting $B=n^{0.6}$.

To check why the Pearson coefficient shows higher dependence over the MIC, contrary to references recommended in other research fields, the following two aspects are discussed: (1) the influence of threshold B on the MIC; (2) the effect of noise on the MIC.

The selection of threshold B, relating to meshing accuracy, is a comprehensive consideration of the calculation accuracy and computational efficiency, and has a certain relationship with the length of datasets. To explore the influence of threshold B on MIC and choose the appreciated B, two independent random variables with 6120 points, consistent with the sample size of the cable force trend in this paper, are adopted. The four symbols in Fig. 5 represent the MIC values when $B=n^{0.6}$, $B=n^{0.7}$, $B=n^{0.8}$, and $B=n^{0.9}$, respectively. As can be seen from Fig. 5, the MIC for the two independent variables is less than 0.1 when $B=n^{0.6}$; but close to 0.6 when $B=n^{0.9}$. Considering the basic principal of the MIC, that a reasonable meshing accuracy B should ensure the MIC is close to 0 for two independent variables (Reshef *et al*. 2011), the default selection of B is reasonable for a cable force trend with 6120 data length.

A specific linear relationship with different levels white noise is employed to investigate the influence of noise on the MIC, and the simulation of noise refers to Law and Li (2010) and Ding *et al.* (2017). The comparison between the MIC and Pearson coefficients is shown in Fig. 6. Obviously, the MIC and Pearson correlation decreased with the noise level increase. However, the MIC shows to be much more sensitive to noise, which can undermine the MIC advantage in measuring the association between variables. The above viewpoint has also been confirmed by Gorne *et al*. (2015) and Simon and Tibshirani (2014) through simulation, which emphasised that the MIC has a good statistical effect for ideal non-noise or noiseless variables.

However, for monitored cable force trend datasets, the scatter plot of two symmetrical cable forces is shown in Fig. 7. A clear linear relationship can be observed, meanwhile, an obvious characteristic in the distribution of "wide-band' can also be obtained. The real operation conditions of a certain noise level lead to adverse effects on the MIC. Moreover, the MIC fails to measure the correlation in monitored cable forces for the investigated bridge in this study.

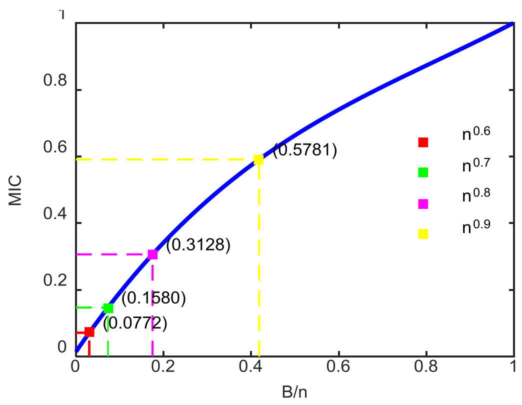

Fig. 5 MIC of random variables for different *B*

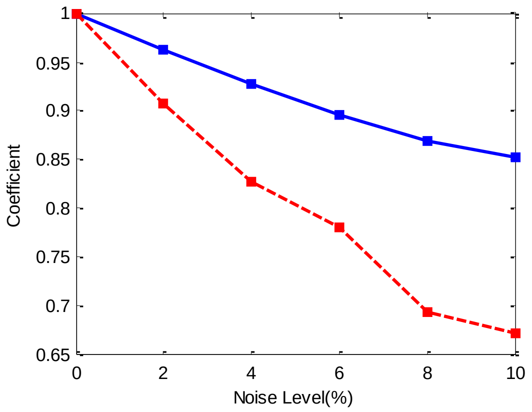

Fig. 6 MIC and Pearson correlation coefficient for different noise

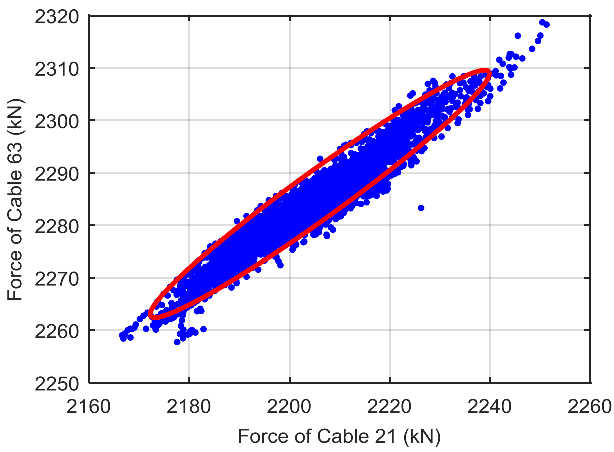

Fig. 7 Characteristic of “Wide-band” of cable tension

2.3 Spatial correlation analysis using MI

MI, as a fundamental quantity in information theory, was first proposed in 1951 by Shannon (1951) in the field of discrete systems. Mutual information, *MI* (*A*,*B*), measures the uncertainty reduction of variable A given that B has been observed (Tourassi *et al.* 2001). Therefore, MI is considered a natural and general tool for quantifying statistical association between pairs of variables. The MI between two discrete random variables A and B is defined in terms of Shannon entropy as

$$MI(A,B)=H(A)+H(B)-H(A,B)=\sum_i\sum_j p(a_i,b_j)\log\frac{p(a_i,b_j)}{p(a_i)p(b_j)}\geq 0 \tag{4}$$

where $H(\cdot)$ and $P(\cdot)$ indicates the entropy and probability density of variables. The kernel density estimation (Moon *et al.* 1995, Steuer *et al*. 2002) with high precision and an acceptable computational complexity is adopted in this paper to investigate the dependence of different cables.

The Pearson coefficient and MI coefficients of cable pairs in upstream is shown in Fig. 8(a). Different from the MIC shown in Fig. 3, MI has good performance in detecting

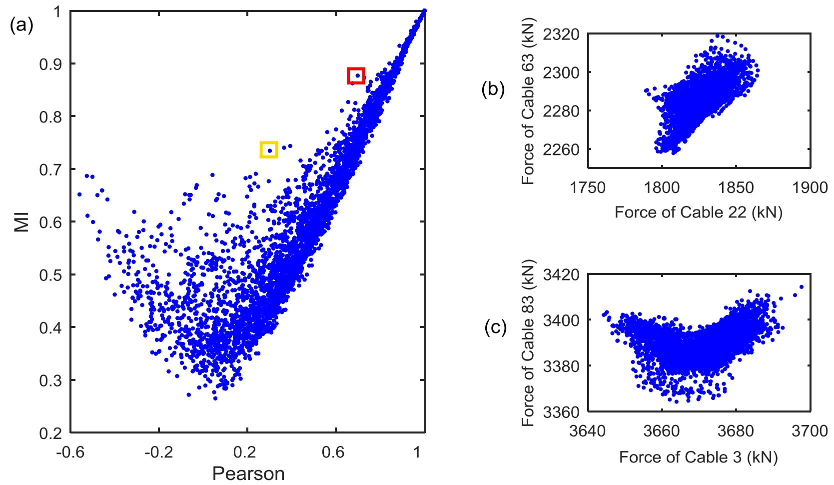

(a) Scatter plot with Pearson and MI

(b) Force of Cable 22 and Cable 63
(c) Force of Cable 3 and Cable 83

Fig. 8 Contrast of correlation coefficient between MI and Pearson

potential association for MI coefficients that are generally greater than the Pearson coefficient, especially for some variables with relative high nonlinearity. For example, a strong correlation could not be generated between Cable 22 and Cable 63 using the scatter plot and Pearson coefficient (0.697), as shown in Fig. 8(b), but a relatively high MI coefficient 0.877 illustrates the internal association between the two cables. In addition, a stronger contrast appears in Cable 3 and Cable 83, as shown in Fig. 8(c). There, the Pearson coefficient was 0.3007, but MI was 0.7345.

Compared with the popular MIC and Pearson coefficient, MI is considered much more suitable for exploring latent relevance between monitored cable force datasets, not only for linear, but also non-linear relationships. Therefore, MI based on kernel density estimation is adopted in this paper, which provides an important prerequisite for subsequent sensor placement optimisation.

In this study, M_{ij} represents the MI between the cable i and cable j, the correlation matrix $\mathbf{I}$ of investigated cables can be expressed as $\mathbf{I}=\left[MI_{ij}\right]_{84\times 84}$. Then, an equivalent correlation matrix $\mathbf{D}=\left[D_{ij}\right]_{84\times 84}$ can be transformed from the correlation matrix $\mathbf{I}$ by binary processing. If $MI_{ij}\geq k$, $D_{ij}=1$; otherwise, $D_{ij}=0$. k indicates the selected correlation threshold.

3. Optimal sensor placement based on Bond Energy Algorithm

3.1 Bond energy algorithm and principal of optimal sensor placement

The purpose of the bond energy algorithm (BEA) is to identify and explore natural variable groups and clusters that occur in complex data arrays (Mccormick and Others, 1969). BEA seeks to uncover the associations and interrelations existing in an array by permuting the rows and columns. As a clustering approach, the BEA starts with an equivalent correlation matrix ($\mathbf{D}=\lfloor D_{ij}\rfloor_{n\times n}$) and transforms $\mathbf{D}$ to a cluster association matrix (CA) by maximising the measure of effectiveness (ME). The ME for an array $A\in R^{M\times N}$ can be expressed as

$$ME(A)=\frac{1}{2}\sum_{i=1}^{M}\sum_{j=1}^{N}a_{ij}\times\left(a_{i,j+1}+a_{i,j-1}+a_{i+1,j}+a_{i-1,j}\right) \quad (5)$$

As can be seen from Eq. (5), ME is chiefly affected by the concentration of larger values in the array. As most elements in the left, right, top, and bottom of equivalent correlation matrix $\mathbf{D}$ are empty, thus, the constraint condition is defined as

$$a_{0,j}=a_{M+1,j}=a_{i,0}=a_{i,N+1}=0 \quad (6)$$

It is remarkable that row and column transform of equivalent correlation matrix $\mathbf{D}$ is equivalent in bond energy algorithm, due to the symmetry of correlation matrix of cable group. Thus, only one dimension of $\mathbf{D}$ is needed to perform such transform, flaw chart of which is illustrated in Fig. 9.

The cluster association matrix (CA) can be obtained by BEA, composed of several sub-matrices arranged along the diagonal, implying group positions with strong correlation.

The CA matrix has block division characteristics, for only the elements in these sub-matrices are equal to 1 and other elements in the matrix are equal to 0. Such block division characteristics shed light on exploring potential relationships between cables and determining optimal sensor placement. Cable positions can be divided into the following five categories according to the arrangement of the sub-matrix: if there is only one element in a sub-matrix, the corresponding positions belong to ***Type 1***; if there is only one element in the intersection of two or more sub-matrices, the corresponding sensor positions belong to ***Type 2***; if there is more than one element in a sub-matrix, and all

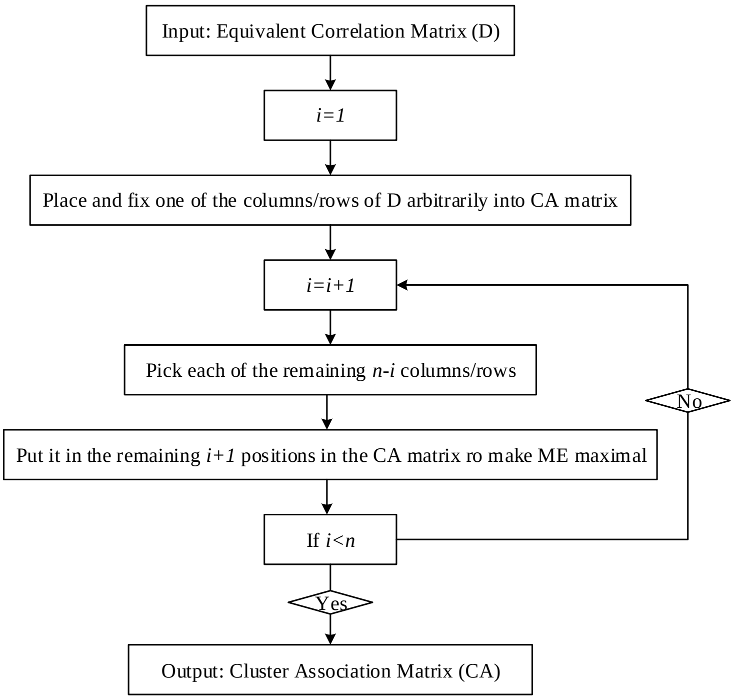

Fig. 9 Flow chart of bond energy algorithm

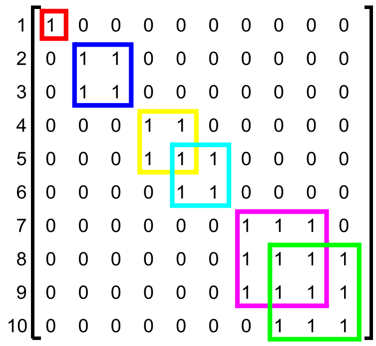

Fig. 10 Clustering Association matrix scheme (CA)

the elements in matrix do not intersect with other sub-matrices, the corresponding sensor positions belong to ***Type 3***; if there is more than one element in the intersection of two or more sub-matrices, the corresponding sensor positions belong to ***Type 4***; Other sensor position in the matrix belong to ***Type 5***.

Take the CA matrix shown in Fig. 10 as an example. Position 1 and 5 belong to ***Type 1***, ***Type 2***, respectively; positions 2 and 3 belong to ***Type 3***; positions 8 and 9 belong to ***Type 4***; positions 4, 6, 7, and 10 belong to ***Type 5***. The optimal sensor placement can be conducted using cable position categories following the principle of selecting representative sensors. Detailed information for the bond energy algorithm and sensor selecting principal can be found in the co author's reference (Lu *et al*. 2016).

3.2 Optimal sensor placement with threshold k=0.9

When applying the spatial correlation analysis and bond energy algorithm to the 84 investigated cables on the upriver side of the Nanjing No.3 Yangtze River Bridge, the equivalent correlation matrix can be obtained by binary processing, employing the threshold $k=0.9$. 50 sub-matrices clustered by BEA are distinguished by boxes of different colours in Fig. 11, explicitly illustrating the correlation in the cable group, whose marshalling sequence determines the sensor position classification.

The 72 potential optimal sensor placements, generated from the 84 cable positions, is shown in Table 1. According to the principle of selecting representative sensors (Lu *et al.* 2016), all the cable positions in ***Type 1*** and ***Type 2*** categories, the number of which are m_1 and m_2, respectively, are first chosen as optimal monitoring points. If the number of cable positions in ***Type 3*** and ***Type 4*** categories are m_3 and m_4 (6 and 3 in this study), one position should be

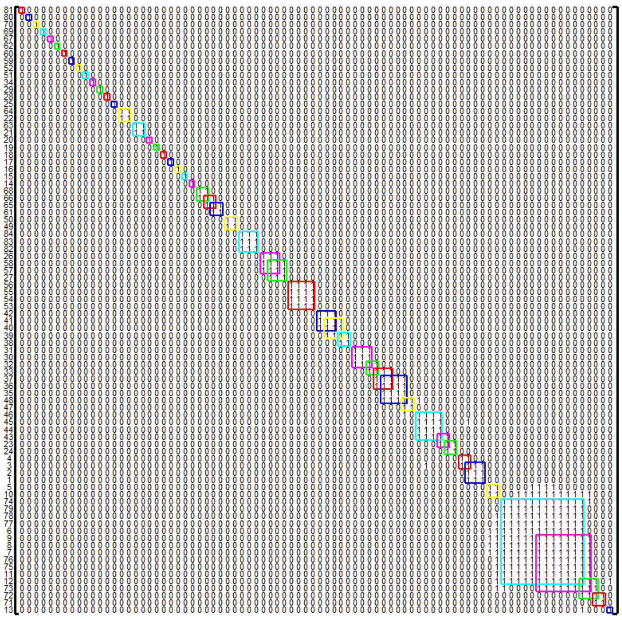

Fig. 11 Clustering correlation matrix of cable group when k=0.9

Table 1 Classification of cable positions

Category	Cable Position	Total
Type 1	13,14,15,16,17,18,19,20,25,28,29,34,51,52,59,60,62,67,69,70,80,81	22
Type 2	3,12,23,32,33,39,43,48,65,66,72	11
Type 3	{5,10},{21,63},{22,64},{49,50},{53,54,55,56},{82,83,84}	6
Type 4	{36,37},{40,41},{57,58}	3
Type 5	Other positions	30

selected as optimal monitoring point from each intersection. So the total number of optimal sensor placements from these four categories is $m' = m_1 + m_2 + m_3 + m_4$ (42 in this study). The positions at the ***Type 5*** categories are usually correlated with positions at the ***Type 2*** or ***Type 4*** categories, and such positions are neglected for potential optimal sensor positions. Thus, the number of possible combinations for optimal sensor positions depends on the potential sensor placements within ***Type 3*** and ***Type 4*** categories. In this study, the number of total combinations could be calculated as $\underbrace{C_2^1 \cdot C_2^1 \cdot C_2^1 \cdot C_2^1 \cdot C_4^1 \cdot C_3^1}_{\text{Type3}} \underbrace{C_2^1 \cdot C_2^1 \cdot C_2^1}_{\text{Type4}} = 1536$. Moreover, the average correlation degree is employed to determine the most reasonable combination among all these combinations, which is defined as the sum of correlation coefficients (MI in this study) of all potential optimal sensor positions

$$\bar{I} = \frac{1}{m'^2} \sum_{i=1}^{m'} \sum_{j=1}^{m'} MI_{ij} \tag{7}$$

The average correlation degree of each combination is shown in Fig. 12. The minimum average correlation degree is 0.563 and the corresponding combination, consisting of positions {64,63,50,84,58,55,41,36,10} is selected for optimal monitoring positions. The optimal sensor placement checking process shows that cable positions 33 and 32 are in the same submatrix. Thus, cable position 33 is superfluous and eliminated in the final optimisation results.

The final optimal monitoring positions are demonstrated in Fig. 13. It can be seen from Fig. 13 that: (1) the final optimal scheme only contains 41 cable force monitoring positions, almost half of the investigated cables, which greatly reduced the number of sensors and proved the effectiveness of the method; (2) symmetrical positions like {21,63} and {22,64}, as well as adjacent positions like {53,54,55,56} and {82,83,84} are found in intersections in the ***Type 3*** category for the potential optimal monitoring point, proving that the clustering results based on the spatial correlation analysis is consistent with the previous empirical experience; (3) the optimal points near the tower are more dense, indicating that the cable tension of short cables have a large difference from each other, more sensors should be installed to get a comprehensive understanding of the cable force there. For long cables far away from the tower, fewer sensors need to be installed, indicating an obvious correlation between long cables; (4) the optimal sensor placement was not strictly symmetrical, implying the non-stress length differences of cables and non-uniform distribution of temperature loads.

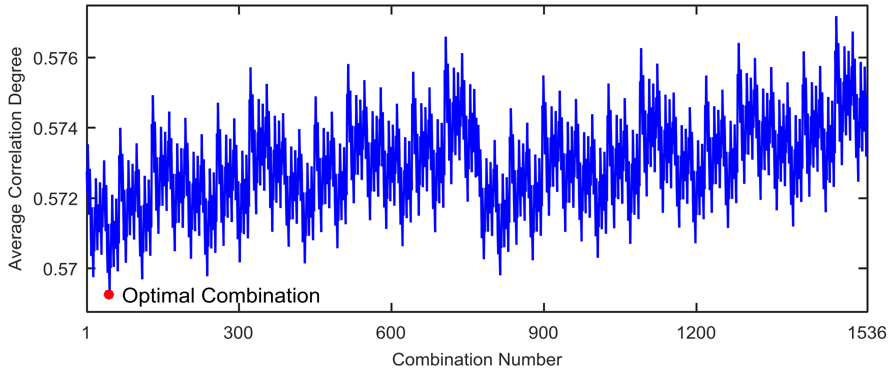

Fig. 12 Average correlation degree of potential optimal position combinations

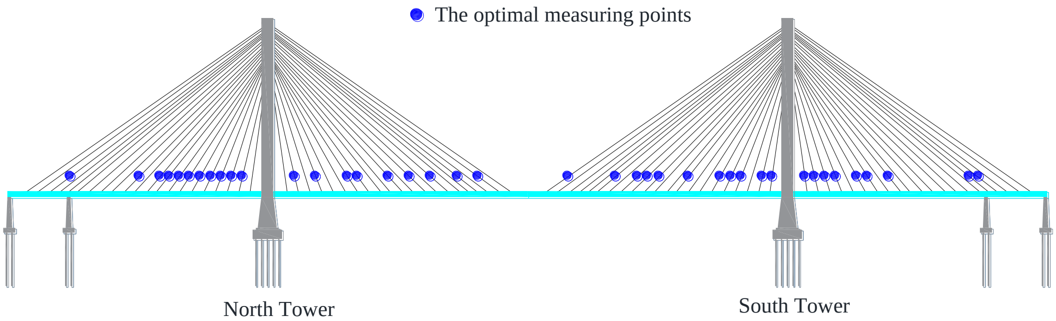

Fig. 13 Optimal sensor placement when k=0.9

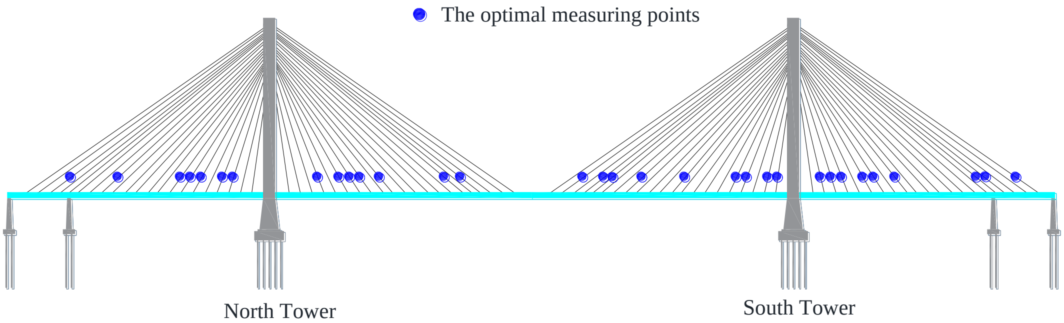

Fig. 14 Optimal sensor placement when k=0.85

3.3 Comparison of optimal sensor placement with different threshold

When the threshold k=0.85, there are 42 sub-matrices arranged along the diagonal in the clustering correlation matrix. The classification of 84 cable positions is shown in Table 2 and number of combinations for potential monitoring points from ***Type 3*** and ***Type 4*** categories is $\underbrace{C_2^1 \cdot C_4^1 \cdot C_3^1}_{Type3} \underbrace{C_5^1 \cdot C_2^1 \cdot C_2^1 \cdot C_2^1 \cdot C_2^1 \cdot C_2^1 \cdot C_2^1 \cdot C_2^1}_{Type4} = 15360$. A total of 32 optimal monitoring positions can be obtained through minimising the average correlation degree shown in Fig. 14.

The optimal sensor placement using the Pearson coefficient matrix $\mathbf{R} = \left[Corr_{ij}\right]_{n\times n}$ can also be conducted in the same way. Table 3 summarizes the optimal monitoring positions using different thresholds and different correlation analysis methodology. It can be seen from Table 3 that the number of optimal monitoring positions, obtained through MI and Pearson coefficients, increased with the correlation threshold increase. Moreover, the number of optimal points generated by the MI based method is always less than that

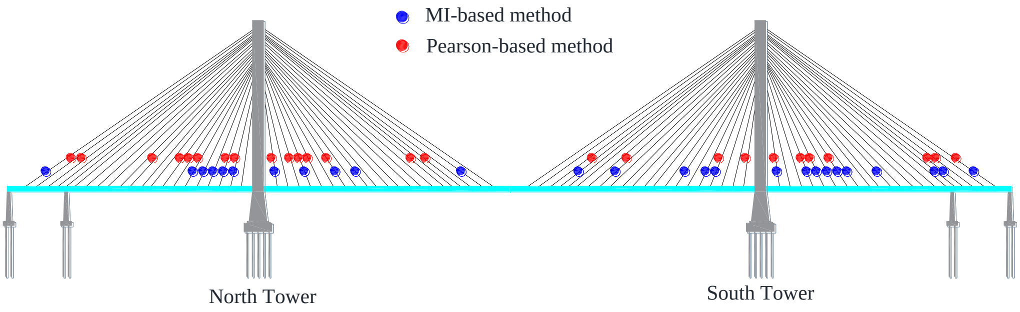

Fig. 15 Optimal sensor placement for two spatial correlation analysis methods

Table 2 Classification of cable positions

Category	Cable Position	Total
Type 1	16,18,19,25,28,29,47,59,60,62,67,69,70,72,80,81	16
Type 2	3,14,44,46,48,54,56,65	8
Type 3	{15,17},{26,27,57,58},{82,83,84}	3
Type 4	{7,8,9,11,12},{22,63},{30,31},{33,37},{39,40},{41,42},{49,50},{61,66}	8
Type 5	Other positions	32

Table 3 Number of optimal monitoring positions

Threshold	0.9	0.85	0.8	0.75	0.7	0.65	0.6
Mutual information	41	32	26	22	16	15	13
Pearson coefficient	48	35	30	26	22	18	17

of the Pearson based method with the same threshold, which is inseparable from the fact that the mutual information can not only describe the linear, but also nonlinear relationship between cable forces. The minimum number of optimal monitoring positions settled around 16 in both methods when choosing a strong correlation threshold $k \geq 0.06$, reflecting at a certain extent, that at least 16 cable sensors should be installed on the Nanjing Yangtze River Bridge to obtain a comprehensive knowledge of cables in the upstream. However, the choice of threshold or number of optimal sensor positions is also significantly influenced by the accuracy, budget, and even the administrative authority.

The comparison of optimal sensor placements making use of the MI with threshold k=0.8 and Pearson coefficient with threshold k=0.75 is shown in Fig. 15 (with same optimal sensor number), revealing a similar regulation that points are more intensive among the short cables close to the tower, and sparse among long cables. More than 50% of optimal sensor positions are arranged on the same cable.

For optimal sensor placement based on spatial correlation, the most important issue is the correlation matrix determination. Usually there are two approaches, generated from a finite element model or from monitoring datasets. The monitoring system provides the actual structure response under actual environmental and load conditions. The correlation matrix calculated from long-term monitored cable forces will provide guidelines for the same type bridges.

4. Conclusions

Reasonable sensor placement is crucial and essential for establishing and maintaining a cost-effective structural health monitoring system and obtaining the necessary structural response data to precisely evaluate the state of the bridge. This paper investigates the spatial correlation between monitored cable forces and employs the bond energy algorithm to conduct optimal sensor placement using a correlation matrix. The following conclusions are obtained:

- The Pearson correlation coefficient, MIC, and MI are employed to investigate the deep spatial correlation in the monitored cable forces. In addition, the MI shows certain superiority over the other two measures, and explores the linear and nonlinear spatial correlation in cable forces, which provides a solid basis for reasonable sensor placement optimisation.

- Several schemes of sensor arrangement with different thresholds, using the BEA algorithm, were discussed. The number of optimal sensors calculated by the MI-based method is less than that of the Pearson-based method under the same threshold. Further, the optimal sensor points are more intensive among the short cables, while sparse among long cables

In practice, the optimal cable force monitoring points are often difficult to determine or justly determined by virtue of experience. The presented approach incorporates monitored cable forces that will lead to a better understanding of spatial correlation between cables and reasonable sensor monitoring locations, which will shed light on the safety assessment and decision making process in the future.

It should be noted that dead load and temperature load induced cable force has been employed in the proposed optimal sensor placement method, while vehicle load, playing a significant role in cable force variation, has not been considered for inherent complicated relevance. Optimal sensor placement utilizing vehicle load induced cable force would be discussed in the near future.

Acknowledgments

The research described in this paper was financially supported by National Natural Science Foundation of C hina (NSFC Grant No. 51478149, 51678204, 51638007) and the 973-Program project (No. 2013CB036305).

References

Allemang, R.J. and Brown, D.L. (1982),"A correlation coefficient for modal vector analysis", *Proceedings of the 1st international modal analysis conference*, SEM, Orlando, USA, January.

Baruh, H. and Choe, K. (1987), "Sensor-failure detection method for flexible structures", *J. Guid. Control Dynam.*, **10**(5), 474-482.

Carne, T.G. and Dohrmann, C. (1994), "A modal test design strate gy for model correlation", *Proceedings of the SPIE - The International Society for Optical Engineering*, Nashville, USA, December.

Dewolf, J.T. and Zhao, J. (1999), "Sensitivity study for vibrational parameters used in damage detection", *J. Struct. Eng.*, **125**(4), 410-416.

Ding, Z.H., Lu, Z.R. and Liu, J.K. (2017), "Parameters identificati on of chaotic systems based on artificial bee colony algorithm c ombined with cuckoo search strategy", *Sci. China Technol. Sci.*, 1-10.

Doebling, S.W. (1995), "Measurement of structural flexibility matrices for experiments with incomplete reciprocity", *Proceedings of the International Symposium on Physical Design*, Japan, January.

Gorfine, M., Heller, R. and Heller, Y. (2015), Comment on "Detecting Novel Associations in Large Data Sets", *Eprint Arxiv*.

Guyan, R.J. (1965), "Reduction of stiffness and mass matrices", *Aiaa J.*, **3**(2), 380-380.

Jemielniak, K. (1999), "Commercial tool condition monitoring systems", *Int. J. Adv. Manufact. Tech.*, **15**(10), 711-721.

Jung, B.K., Cho, J.R. and Jeong, W.B. (2016), "Reproduction of vibration patterns of elastic structures by block-wise modal expansion method (bmem)", *Smart Struct. Syst.*, **18**(4), 819-837.

Kammer, D.C. (1991), "Sensor placement for On-Orbit modal identification and correlation of large space Structures", *Proceedings of the American Control Conference, Boston*, USA, June.

Law, S.S. and Li, J. (2010), "Updating the reliability of a concrete bridge structure based on condition assessment with uncertainties", *Eng. Struct.*, **32**(1), 286-296.

Li, D., Li, H. and Fritzen, C. (2007), "The connection between effective independence and modal kinetic energy methods for sensor placement", *J. Sound Vib.*, **305**(4-5), 945-955.

Li, D., Zhou, Z. and Ou, J. (2011), "Development and sensing properties study of FRP–FBG smart stay cable for bridge health monitoring applications", *Measurement*, **44**(4), 722-729.

Li, H., Ou, J. and Zhou, Z. (2009), "Applications of optical fibre Bragg gratings sensing technology-based smart stay cables", *Opt. Laser. Eng.*, **47**(10), 1077-1084.

Lim, K.B. (2012), "Method for optimal actuator and sensor placement for large flexible structures", *J. Guid. Control Dynam.*, **15**(1), 49-57.

Liu, W., Gao, W.C., Sun, Y. and Xu, M.J. (2008), "Optimal sensor placement for spatial lattice structure based on genetic algorithms", *J. Sound Vib.*, **317**(1), 175-189.

Lu, L., Wang, X., Liao, L., Wei, Y., Huang, C. and Liu, Y. (2015), "Application of model reduction technique and structural subsection technique on optimal sensor placement of truss structures", *Smart Struct. Syst.*, **15**(2), 355-373.

Lu, W., Wen, R., Teng, J., Li, X. and Li, C. (2016), "Data correlation analysis for optimal sensor placement using a bond energy algorithm", *Measurement*, **91**, 509-518.

Mccormick, W.T. Jr. and Others, A. (1969), "Identification of data structures and relationships by matrix reordering techniques", *Algorithms*, **141**.

Mehrad, V., Xue, D. and Gu, P. (2013), "Prediction of surface reconstruction uncertainties for freeform surface inspection", *Measurement*, **46**(8), 2682-2694.

Moon, Y.I., Rajagopalan, B. and Lall, U. (1995), "Estimation of mutual information using kernel density estimators", *Physical Review E Statistical Physics Plasmas Fluids & Related Interdisciplinary Topics*, **52**(3), 2318-2321.

Nestorovic, T., Trajkov, M. and Garmabi, S. (2015), "Optimal placement of piezoelectric actuators and sensors on a smart beam and a smart plate using multi-objective genetic algorithm", *Smart Struct. Syst.*, **15**(4), 1041-1062.

Penny, J., Friswell, M. and Garvey, S. (1994), "Automatic choice of measurement locations for dynamic testing", *AIAA J.*, **32**(2), 407-414.

Reshef, D.N., Reshef, Y.A., Finucane, H.K., Grossman, S.R., Mcvean, G., Turnbaugh, P.J., Lander, E.S., Mitzenmacher, M. and Sabeti, P.C. (2011), "Detecting novel associations in large datasets", *Science*, **334**(6062), 1518.

Shannon, C.E. (1951), "A mathematical theory of communication", *The Quarterly Review of Biology*, **26**(3), 3-55.

Simon, N. and Tibshirani, R. (2014), "Comment on "Detecting Novel Associations In Large Data Sets" by Reshef *et al.*, Science Dec 16, 2011", *Statistics*.

Speed, T. (2011), "A correlation for the 21st century", *Science*, **33 4**(6062), 1502-1503.

Steuer, R., Kurths, J., Daub, C.O., Weise, J. and Selbig, J. (2002), "The mutual information: detecting and evaluating dependencies between variables", *Bioinformatics*, 18 Suppl 2(suppl_2), S231-240.

Tong, K.H., Yassin, A.Y.M., Bakhary, N. and Kueh, A.B.H. (2014), "Optimal sensor placement for mode shapes using improved simulated annealing", *Smart Struct. Syst.*, **13**(3), 389-406.

Tourassi, G.D., Frederick, E.D., Markey, M.K. and Floyd Jr., C.E. (2001), "Application of the mutual information criterion for feature selection in computer-aided diagnosis", *Medical Phys.*, **28**(12), 2394.

Udwadia, F.E. (2010), "Methodology for optimum sensor locations for parameter identification in dynamic systems", *J. Eng. Mech.*, **120**(2), 368-390.

Waldraff, W., Dochain, D., Bourrel, S. and Magnus, A. (1998), "On the use of observability measures for sensor location in tubular reactor", *J. Process Control*, **8**(5-6), 497-505.

Wang, M.L., Satpathi, D., Koontz, S., Jarosevic, A. and Chandoga, M. (1999), "Monitoring of cable forces using magneto-elastic sensors", *Comput. Mech. Struct. Eng.*, 337-347.

Yang, Y. and Nagarajaiah, S. (2013), "Blind modal identification of output-only structures in time-domain based on complexity pursuit", *Earthq. Eng. Struct. D.*, **42**(13), 1885-1905.

Yang, Y. and Nagarajaiah, S. (2013), "Output-only modal identification with limited sensors using sparse component analysis", *J. Sound Vib.*, **332**(19), 4741-4765.

Yang, Y. and Nagarajaiah, S. (2014), "Structural damage identification via a combination of blind feature extraction and sparse representation classification", *Mech. Syst. Signal Pr.*, **45**(1), 1-23.

Yao, L., Sethares, W.A. and Kammer, D.C. (1992), "Sensor placement for on-orbit modal identification of large space structure via a genetic algorithm", *Proceedings of the IEEE International Conference on Systems Engineering*, Kobe, Japan, September.

Yi, T.H., Li, H.N., Gu, M. and Zhang X.D. (2015), "Sensor placement optimization in structural health monitoring using niching monkey algorithm", *Smart Struct. Syst.*, **15**(1), 191-207.

Yi, T.H., Zhou, G.D., Li, H.N. and Zhang, X.D. (2015), "Optimal sensor placement for health monitoring of high-rise structure based on collaborative-climb monkey algorithm", *Struct. Eng. Mech.s*, **54**(2), 305-317.

Zhou, G.D., Yi, T.H., Zhang, H. and Li, H.N. (2015), "Optimal nsor placement under uncertainties using a nondirective ent glowworm swarm optimization algorithm", *Smart Struct. Syst*, **16**(2), 243-262.

CC